Intelligent Reflecting Surface Based Backscatter Communication for Data Offloading

Sai Xu, *Member, IEEE,* Yanan Du, *Graduate Student Member, IEEE,*
Jiajia Liu, *Senior Member, IEEE,* and Jingtao Li

***Abstract*—This paper investigates intelligent reflecting surface based backscatter communication (IRS-BackCom), in order to realize computational task offloading of energy-constrained mobile edge computing network in a self-sustainable manner. Specifically, the system operation is divided into two phases. In the first one, the ambient signal energy from a power beacon (PB) either provides the energy supply of local computing and energy harvesting circuits, or flows into the energy storage, when reaching the IRS. In the second one, the stored energy is used to enable IRS-BackCom for partial computational data offloading and energize local computing circuit. Based on this, the maximization problem of sum computational bits is formulated. By jointly optimizing the beamforming vector at the PB, the backscatter matrix at the IRS, the time scheduling of two-phase process, as well as the time of local computing, sum computational bits are maximized. In addition, this paper proposes element clustering to realize BackCom, so as to reduce the control and computation complexity of IRS. According to different operating mechanisms, two cluster operation modes are considered, namely independent cluster operation mode and joint cluster operation mode. Simulation results demonstrate the achievable sum computational bits by the proposed IRS-BackCom schemes.**

***Index Terms*—Intelligent reflecting surface (IRS), backscatter communication (BackCom), energy harvesting (EH), mobile edge computing (MEC), element clustering.**

I. Introduction

UBIQUITOUS Internet-of-Things (IoT) applications have penetrated into various aspects of human lives, such as industrial or agriculture monitoring, intelligent transportation, automatic navigation, home automation, health care, etc. For many IoT services, computation- and latency-sensitive tasks are often involved, which unusually require powerful computation capability [1]. Nevertheless, most IoT devices have rather limited computing power because of stringent cost and size consideration. On the other hand, severely restricted energy supply due to finite battery capacity is widely believed to be another serious impediment to the expansion of potential IoT services in practice. Currently, there is an urgent need to exploit the methods of utilizing computation- and energy-constrained IoT devices to meet increasing resource-hungry applications [2].

To handle the challenges posed by data processing, mobile edge computing (MEC) techniques have been extensively investigated. The core idea of MEC techniques is to offload data processing tasks to the surrounding MEC server having powerful computation capacity, based on which the tasks can be completed more quickly and the computation latency is reduced [3]. According to whether partial or full computational data is offloaded, MEC networks are often classified into two modes [4]. The first one is termed as partial computation offloading. In some scenarios, a computation task can split into two parts. Using the mode of partial computation offloading, they are separately processed through local computing and data offloading. The second one is named after binary computation offloading [5]. In other scenarios, it is unrealistic to partition a computation task. Adopting the mode of binary computation offloading, such a task is either locally computed or entirely offloaded to MEC servers [6].

For mitigation of adverse effects of limited energy supply, energy harvesting (EH) techniques have attracted much attention [7], [8]. The techniques aim to harvest ambient radio frequency (RF) signals to supply the energy consumption of wireless devices [9]. Clearly, the development of EH provides an optional way for data offloading in low-consumption IoT. With the integration of MEC and EH, a novel paradigm, namely wireless powered MEC, is spawned. Wang *et al.* [10] investigated a single-user wireless powered MEC system. Relying on the harvested energy, computation task allocation for local computing and data offloading and transmission energy allocation were optimized to minimize the total transmit power. Bi and Zhang [11] considered a multi-user wireless powered MEC network in the mode of binary computation offloading. By jointly optimizing binary decision-making and the time scheduling, the weighted sum computation rate was maximized.

By exploiting EH to harvest wireless energy, the shortage of energy consumption is alleviated to some extent. Nevertheless, it is often inadequate for power-hungry tasks to rely only

This work was supported in part by Project funded by the China Postdoctoral Science Foundation (2021M692649); in part by the National Natural Science Foundation of China (62101448); in part by European Commission's Horizon 2020 MSCA Individual Fellowship SICIS under Grant (101032170); in part by the Fundamental Research Funds for the Central Universities (D5000210593); in part by Basic Research Programs of Taicang, 2020 (TC2020JC06).

S. Xu (e-mail: xusai@nwpu.edu.cn) is with the School of Cybersecurity, Northwestern Polytechnical University, Xi'an, Shaanxi, 710072, China, and also with the Department of Electronic and Electrical Engineering, University of Sheffield, Sheffield, S1 4ET, UK. Y. Du (e-mail: ynduyndu@163.com) is with the College of Intelligent Systems Science and Engineering, Harbin Engineering University, Harbin, Heilongjiang, 150001, China. J. Liu (e-mail: liujiajia@nwpu.edu.cn) (the corresponding author) is with the School of Cybersecurity, Northwestern Polytechnical University, Xi'an, Shaanxi, 710072, China. J. Li (e-mail: lijingtao216@sohu.com) is with the Beijing Institute of Technology, Beijing, 100081, China, and also with the Institute of Telecommunication and Navigation Satellites, China Academy of Space Technology, Beijing, China.

Manuscript received XX XX, XXXX; revised XX XX, XXXX.

on EH techniques. To further reduce energy consumption and raise energy efficiency, backscatter communication (BackCom) techniques are developed in a wireless powered MEC network. By modulating ambient wireless signal, new data from a backscatter transmitter is able to overwrite the original data carried by the signal [12]. Gong *et al.* [13] proposed to customize deep reinforcement learning to maximize energy efficiency in data offloading. Zou *et al.* [14] investigated BackCom-based wireless powered MEC sensor networks and minimized the total energy consumption. Shi *et al.* [5] considered a practical non-linear EH model and maximized the weighted sum computational bits of edge users. Ye *et al.* [15] studied delay minimization in a hybrid wireless powered MEC network leveraging BackCom and active transmissions (AT) simultaneously. Xu *et al.* [16] minimized the total energy consumption of wireless devices in a wireless powered BackCom-based MEC network by allocating computation offloading and wireless resource. Nguyen *et al.* [2] investigated OFDMA-based wireless powered MEC using BackCom.

By integrating MEC, EH and BackCom techniques, a wireless powered self-sustainable system of data offloading can be realized. Recently, rapid development of intelligent reflecting surface (IRS) [17], [18] offers an excellent opportunity to upgrade the level of such a system, since it is able to significantly augment the performance of BackCom and EH. Being a programmable two-dimensional metasurface [19]–[21], IRS consists of a great many passive elements, which can collaborate to effectively control the reflection property of the incoming electromagnetic (EM) wave. Owing to low price, low power consumption, easy scalability and high-level degree of spatial freedom, IRS is often employed to enhance signal reception as well as communication security and covertness [22]–[24]. With the advance of IRS techniques, MEC and BackCom have entered into a new stage. Bai *et al.* [25] investigated IRS-aided MEC networks, and latency-minimization problems were formulated and solved. Furthermore, wireless powered IRS-aided MEC was studied [26]. When IRS was integrated with BackCom, Yan *et al.* [27] proposed to employ BackCom to simultaneously enhance the primary communication and send the new private data to the receiver. Zhao *et al.* [28] investigated the performance of backscatter link and direct link in IRS-assisted communications. In [29], [30], IRS-based BackCom (IRS-BackCom) was employed to convert harm into benefit for resisting undesired signal and to improve the transmission security, respectively.

Up to now, existing works have investigated how to apply EH and BackCom techniques to MEC networks. Meanwhile, IRS-aided MEC networks have also been studied, where IRS is used as a reflection device to enhance signal reception. Currently, none of researches have taken into account wireless powered MEC assisted by IRS-BackCom, where IRS acts as a backscatter device. Motivated by this fact, this paper will leverage wireless powered IRS-BackCom to realize data offloading. Such a system is particularly appealing, because it can leverage EH techniques to cover energy expenditure when BackCom with low consumption is employed to offload data bits to an MEC server. Moreover, by integrating IRS into wireless powered backscatter-enabled MEC, introduced inherent spatial diversity can improve communication performance of wireless network beyond all doubt. The main contributions of this paper are summarized as follows.

- To the best of our knowledge, it is the first attempt to apply IRS-BackCom to MEC networks. Distinguished from the conventional BackCom, the introduction of IRS improves degree of spatial freedom and enhances control over EM environment greatly. As a result, the backscatter transmitter for data offloading is upgraded from single-input channel to multiple-input channel. Based on this, multiple MEC servers are considered to exploit the spatial diversity.
- In wireless powered MEC assisted by IRS-BackCom, the maximization problem of sum computational bits is formulated. By jointly optimizing the beamformer at the power beacon (PB), the backscatter matrix at the IRS, the time scheduling of two-phase process, as well as the time of local computing, sum computational bits are maximized. What's more, the computational complexity is analyzed.
- To reduce the control and computing complexity for the IRS comprising a large number of elements, this paper proposes to employ element clustering to realize BackCom, with two cluster operation modes presented, namely independent cluster operation mode and joint cluster operation mode. Then, their computational complexities are also computed.
- Simulations are performed to show how the sum computational bits of system depend on element number of IRS, element cluster number, the transmit power of the PB, the average distance from the IRS to the MEC servers, and the number of the MEC servers. The simulation results demonstrate that the proposed IRS-BackCom schemes can achieve as high sum computational bits as active antennas. Moreover, the IRS-BackCom schemes based on element clustering are capable of achieving quite creditable sum computational bits, while more fine-grained element control of IRS may yield a higher communication performance.

The rest of this paper is structured as follows. In section II, the system model of wireless powered MEC assisted by IRS-BackCom is presented. Then, the maximization problem of sum computational bits is formulated. Section III presents an optimization solution to the maximization problem of sum computational bits. Section IV proposes to employ element clustering to realize rate maximization of BackCom. Section V demonstrates communication performance achieved by the proposed schemes via simulations. Section VI draws the conclusions of this paper.

Notations: In this paper, $\mathbb{R}$ and $\mathbb{C}$ represent the sets of real and complex number, respectively. Let lowercase, boldfaced lowercase and uppercase letters denote scalars, vectors, and matrices, respectively. The notations $(\cdot)^T$, $(\cdot)^H$, $(\cdot)^{-1}$, $\mathrm{tr}(\cdot)$, $|\cdot|$, $\|\cdot\|$ and $\mathrm{Re}(\cdot)$ represent transposition, conjugate transpose, inversion, trace, modulus, Euclidean norm or Frobenius norm, real part of the arguments, respectively. $\succeq$ is a positive

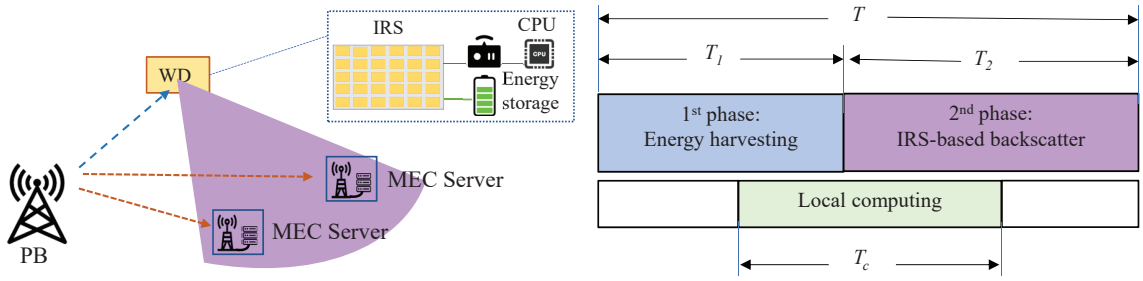

(a) IRS-based backscatter communication (b) Time scheduling of two-phase process

Fig. 1. An illustration of wireless powered MEC model, where IRS-based backscatter communication is employed for data offloading.

semidefinite operator. diag$\{\mathbf{x}\}$ is the diagonal matrix having the entries of $\mathbf{x}$ on its main diagonal.

II. System Model and Problem Formulation

A. System Model

As illustrated in Fig. 1, a self-sustainable wireless powered MEC system is considered, where an N-antenna PB serves as an ambient RF source to supply a wireless device (WD) for some computational task processing. The WD is wired together with an L-element IRS, a CPU and an energy storage, which enable separate energy harvesting, local computing and data offloading. It is assumed that each task is comprised of bit-wise independent data bits, thus the WD is capable of offloading its partial data to K single-antenna MEC servers via IRS-BackCom with $K < L$ and $\mathcal{K} = \{1, 2, \cdots, K\}$. Meanwhile, local computing may also be performed for the remaining computational bits [31]. By exploiting the spatial freedom of multiple MEC servers, the performance loss due to channel fading can be reduced. Another assumption is that all channels are reciprocal and follow quasi-static block fading. Moreover, we leave out the task processing time at the MEC servers and the return transmission delay from the MEC servers to the WD.

To better illustrate the operating mechanism of system, only one time block T is here considered, when all channels remain constant. While the PB transmits its energy-bearing signal s during T, the operation of IRS is divided into two phases. In the first phase T_1, the signal energy reaching the IRS is partially used to supply the power consumption of local computing and energy harvesting circuits, while the rest of energy flows into the energy storage. In the second phase T_2, the stored energy is used to supply IRS-BackCom circuit to offload partial data bits and energize local computing circuit. In the whole time block, the starting and ending time of local computing at the WD is uncertain, each of which may occur at any time.

In the first phase, the received signal at the IRS is given by

$$\mathbf{y}_{I,1} = \sqrt{P}\mathbf{H}\mathbf{w}_1 s + \mathbf{n}_I, \tag{1}$$

where P is the transmit power budget at the PB. $\mathbf{H} \in \mathbb{C}^{L\times N}$ denotes the channel gain from the PB to the IRS. $\mathbf{w}_1$ represents the beamformer for the signal s with $\mathbb{E}[|s|^2] = 1$ in the first phase. $\mathbf{n}_I \in \mathbb{C}^{L\times 1}$ is white Gaussian noise at the IRS with $\mathbf{n}_I \sim (\mathbf{0}, \sigma_I^2\mathbf{I})$. In practice, the harvested energy at the IRS is usually a non-linear model, which can be expressed as a non-linear function [4], [32]. Generally speaking, the harvested power rises along with the growth of received power until it is saturated. To approximately characterize the non-linear model and the saturation region of energy harvesting in practice, a two-piece linear harvested energy model is widely adopted [33], [34]. Mathematically, the harvested power is described as

$$P_{\mathrm{h}} = \begin{cases} \chi P_{\mathrm{r}}, & \chi P_{\mathrm{r}} < P_{\mathrm{s}}, \\ P_{\mathrm{s}}, & \text{otherwise}, \end{cases} \tag{2}$$

where χ is the energy harvesting efficiency at the IRS. P_{r} and P_{s} denote the received power and the saturation power, respectively. In this model, it is assumed that P_{s} is much larger than P_{r}. Thus, the total amount of harvested energy at the IRS is linearly proportional to the received power. Ignoring the noise power, the harvested energy at the IRS is given by

$$E = \chi T_1 P \|\mathbf{H}\mathbf{w}_1\|^2. \tag{3}$$

Note that we has subtracted out the power consumption of energy harvesting circuit here.

In the second phase, when the signal s from the PB impinges on the IRS, the received signal at the k-th MEC server is given by

$$y_{k,2} = \sqrt{P}\mathbf{h}_k^H \mathbf{w}_2 s + \sqrt{P}\mathbf{f}_k^H \mathbf{\Theta}\mathbf{H}\mathbf{w}_2 s + n_k, \tag{4}$$

where $\mathbf{w}_2$ represents the beamformer at the PB in the second phase. $\mathbf{\Theta}$ denotes the reflection-coefficient matrix. n_k is white Gaussian noise at the k-th MEC server with $n_k \sim (0, \sigma_k^2)$. $\mathbf{h}_k \in \mathbb{C}^{N\times 1}$ and $\mathbf{f}_k \in \mathbb{C}^{L\times 1}$ denote the channel gains from the PB and the IRS to the k-th MEC server, respectively. Let $\mathbf{f}_k^H \mathbf{\Theta}\mathbf{H}\mathbf{w}_2 s = \boldsymbol{\theta}^H \mathbf{\Phi}_k \mathbf{w}_2 s$, where $\mathbf{\Phi}_k = \mathrm{diag}\{\mathbf{f}_k^H\}\mathbf{H}$ and $\boldsymbol{\theta} = [\mathbf{\Theta}_{1,1}, \mathbf{\Theta}_{2,2}, \cdots, \mathbf{\Theta}_{L,L}]^H$ with $[\cdot]_{l,l}$ representing the l-th diagonal element of matrix. Since the backscatter can be executed at the IRS, the original signal s is modulated to K new information-bearing signals x_k with $\mathbb{E}[|x_k|^2] = 1$. To be precise, the modulation can be mathematically expressed as $\boldsymbol{\theta} s = \sum_{k=1}^K \boldsymbol{\theta}_k x_k$, where $\left[\sum_{k=1}^K \boldsymbol{\theta}_k \boldsymbol{\theta}_k^H\right]_{l,l} \le 1$ holds. Thus, it can be deduced that the received signal at the k-th MEC server can be rewritten as

$$y_{k,2} = \sqrt{P}\mathbf{h}_k^H \mathbf{w}_2 s + \sqrt{P}\left(\sum_{i=1}^K \boldsymbol{\theta}_i^H x_i\right)\mathbf{\Phi}_k \mathbf{w}_2 + n_k. \tag{5}$$

The signal-to-interference-plus-noise-ratio (SINR) at the k-th MEC server is given by

$$\gamma_{k,2} = \frac{|\mathbf{w}_2^H \mathbf{\Phi}_k^H \boldsymbol{\theta}_k|^2}{|\mathbf{h}_k^H \mathbf{w}_2|^2 + \sum_{i=1, i\neq k}^{K} |\mathbf{w}_2^H \mathbf{\Phi}_k^H \boldsymbol{\theta}_i|^2 + \sigma_k^2/P}. \quad (6)$$

As the element number and the phase resolution of IRS increase, the power consumption of IRS grows up. Mathematically, the energy consumption of IRS is described as $T_2 L\mu$, where μ denotes power consumption of one element. By harnessing the wireless energy to offload partial task bits to the MEC servers via IRS-BackCom, the achievable offloading bits for the bandwidth W are given by

$$R_{\mathrm{b}} = T_2 W \sum_{k=1}^{K} \log\left(1 + \gamma_{k,2}\right). \quad (7)$$

On the other hand, the data bits locally executed at the WD and the corresponding energy consumption are respectively given by

$$R_{\mathrm{c}} = \frac{T_{\mathrm{c}} f_{\mathrm{c}}}{C_{\mathrm{c}}}, \quad (8)$$

$$E_{\mathrm{c}} = \varepsilon_{\mathrm{c}} T_{\mathrm{c}} f_{\mathrm{c}}^3, \quad (9)$$

where f_{c} denotes the local computing frequency of the CPU, C_{c} is the required number of CPU cycles when computing one bit and ε_{c} is the energy consumption coefficient of the processor's chip at the WD.

B. Problem Formulation

This paper aims to maximize sum computational bits by jointly optimizing the beamforming vector at the PB, the backscatter matrix at the IRS, the time scheduling of two-phase process, as well as the time of local computing [1]. The optimization problem is formulated as

$$\begin{aligned}
(\mathrm{P1}) \quad \max_{\mathbf{w}_1, \mathbf{w}_2, \boldsymbol{\theta}_k, T_1, T_2, T_{\mathrm{c}}} \quad & R_{\mathrm{b}} + R_{\mathrm{c}}, && (10a)\\
s.t. \quad & \mathrm{Tr}(\mathbf{w}_1 \mathbf{w}_1^H) \leq 1, && (10b)\\
& \mathrm{Tr}(\mathbf{w}_2 \mathbf{w}_2^H) \leq 1, && (10c)\\
& \left[\sum_{k=1}^{K} \boldsymbol{\theta}_k \boldsymbol{\theta}_k^H\right]_{l,l} \leq 1, \forall l \in \mathcal{L}, && (10d)\\
& E \geq T_2 L\mu + E_{\mathrm{c}}, && (10e)\\
& T_1 + T_2 = T, && (10f)\\
& T_1 \geq 0, T_2 \geq 0, 0 \leq T_{\mathrm{c}} \leq T. && (10g)
\end{aligned}$$

Note that the exchange of information between the PB and the IRS is smooth enough, thus they can jointly optimize the parameters $\mathbf{w}_1$, $\mathbf{w}_2$, T_1, T_2 and T_{c} to maximize the sum computational bits.

[1]To design the beamforming vector at the PB and the backscatter matrix at the IRS, it is necessary to acquire the channel state informations from the PB to the IRS, from the PB to the MEC servers and from the IRS to the MEC servers. In [17], [18], [35], many existing channel estimation schemes involving IRS have been summarized and can be used as a reference for channel estimation in the scenario of IRS-BackCom.

III. Maximization of Sum Computational Bits

The problem (P1) is non-convex because of the coupling variables $\mathbf{w}_1$, $\mathbf{w}_2$, $\boldsymbol{\theta}_k$, T_1, T_2 and T_{c} in the objective function and constraints. In the following, we will present a solving procedure, by decomposing the problem (P1) into three tractable optimization problems.

A. Harvested Energy Maximization per Unit Time

In this subsection, we will optimize the beamformer $\mathbf{w}_1$ to harvest the most wireless energy from the PB during T_1. Based on this, more computational bits can be computed locally or offloaded to the MEC servers. Since the harvested energy at the IRS per unit time only depends on the optimization variable $\mathbf{w}_1$, this optimization problem is formulated as

$$\begin{aligned}
\max_{\mathbf{w}_1} \quad & \frac{E}{T_1}, && (11a)\\
s.t. \quad & \mathrm{Tr}(\mathbf{w}_1 \mathbf{w}_1^H) \leq 1. && (11b)
\end{aligned}$$

By invoking spectral decomposition, the Hermitian matrix $\mathbf{H}^H\mathbf{H}$ can be decomposed into $\mathbf{H}^H\mathbf{H} = \mathbf{U}_1^H \mathbf{\Lambda} \mathbf{U}_1$, where $\mathbf{\Lambda}$ is a diagonal matrix with elements equal to the eigenvalues of $\mathbf{H}^H\mathbf{H}$. Let $\mathbf{v}_1 = \mathbf{U}_1 \mathbf{w}_1$. We have $E = \|\mathbf{H}\mathbf{w}_1\| = \mathbf{v}_1^H \mathbf{\Lambda} \mathbf{v}_1$. Then, this problem is equivalent to

$$\begin{aligned}
(\mathrm{P2}) \quad \max_{\mathbf{v}_1} \quad & \mathbf{v}_1^H \mathbf{\Lambda} \mathbf{v}_1, && (12a)\\
s.t. \quad & \mathrm{Tr}(\mathbf{v}_1 \mathbf{v}_1^H) \leq 1. && (12b)
\end{aligned}$$

It is not difficult to derive that the maximum value of the objective function is equal to the maximum diagonal element of $\mathbf{\Lambda}$.

B. Rate Maximization of BackCom

In this subsection, we consider the rate maximization problem of BackCom during T_2. From the problem (P1), it is not difficult to find that R_{c} is only related to the optimization variables $\mathbf{w}_2$ and $\boldsymbol{\theta}_k$ with the exception of T_2. Without regard to T_2, this problem can be equivalently reformulated as

$$\begin{aligned}
\max_{\mathbf{w}_2, \boldsymbol{\theta}_k} \quad & \sum_{k=1}^{K} \log\left(1 + \gamma_{k,2}\right), && (13a)\\
s.t. \quad & \mathrm{Tr}(\mathbf{w}_2 \mathbf{w}_2^H) \leq 1, && (13b)\\
& \left[\sum_{k=1}^{K} \boldsymbol{\theta}_k \boldsymbol{\theta}_k^H\right]_{l,l} \leq 1, \forall l \in \mathcal{L}. && (13c)
\end{aligned}$$

In this problem, $\mathbf{w}_2$ and $\boldsymbol{\theta}_k$ are deeply coupled in the objective function and constraints. Moreover, the objective function is a sum of M logarithm functions. Therefore, it is challenging to solve this non-convex optimization problem.

To make it more tractable, Lagrangian dual transform is firstly employed to tackle the logarithm functions. Specifically, introducing auxiliary variables α_k, the logarithm functions are given by

$$\log\left(1 + \gamma_{k,2}\right) = \max_{\alpha_k \geq 0} \log\left(1 + \alpha_k\right) - \alpha_k + \frac{\left(1 + \alpha_k\right)\gamma_{k,2}}{1 + \gamma_{k,2}}. \quad (14)$$

Then, the problem is equivalently expressed as

$$\max_{\mathbf{w}_2,\boldsymbol{\theta}_k,\alpha_k} \quad \sum_{k=1}^{K}\log\left(1+\alpha_k\right)-\alpha_k+\frac{\left(1+\alpha_k\right)\gamma_{k,2}}{1+\gamma_{k,2}}, \tag{15a}$$

$$s.t. \quad \alpha_k \geq 0, \forall k \in \mathcal{K}, \tag{15b}$$

$$\text{(13b) and (13c)}. \tag{15c}$$

Using quadratic transform [36], the objective function of this problem is further expressed as

$$\begin{aligned}
&\sum_{k=1}^{K}\log\left(1+\alpha_k\right)-\alpha_k+\frac{\left(1+\alpha_k\right)\gamma_{k,2}}{1+\gamma_{k,2}}\\
=&\sum_{k=1}^{K}\log\left(1+\alpha_k\right)-\alpha_k+\frac{\left(1+\alpha_k\right)|\mathrm{A}_k|^2}{\mathrm{B}_k}\\
=&\sum_{k=1}^{K}\log\left(1+\alpha_k\right)-\alpha_k\\
&\qquad+\sum_{k=1}^{K}2\sqrt{1+\alpha_k}\mathrm{Re}\{\beta_k^*\mathrm{A}_k\}-\sum_{k=1}^{K}|\beta_k|^2\mathrm{B}_k\\
\triangleq& f(\mathbf{w}_2,\boldsymbol{\theta}_k,\alpha_k,\beta_k),
\end{aligned} \tag{16}$$

where β_k is an auxiliary variable and the superscript $*$ represents the conjugate of scalar. A_k and B_k are given by

$$\mathrm{A}_k=\mathbf{w}_2^H\boldsymbol{\Phi}_k^H\boldsymbol{\theta}_k, \tag{17}$$

$$\mathrm{B}_k=|\mathbf{h}_k^H\mathbf{w}_2|^2+\sum_{i=1}^{K}|\mathbf{w}_2^H\boldsymbol{\Phi}_k^H\boldsymbol{\theta}_i|^2+\sigma_k^2/P. \tag{18}$$

Therefore, the problem is further formulated as

$$\text{(P3)} \quad \max_{\mathbf{w}_2,\boldsymbol{\theta}_k,\alpha_k,\beta_k} \quad f(\mathbf{w}_2,\boldsymbol{\theta}_k,\alpha_k,\beta_k), \tag{19a}$$

$$s.t. \quad \alpha_k \geq 0, \forall k \in \mathcal{K}, \tag{19b}$$

$$\text{(13b) and (13c)}. \tag{19c}$$

The problem (P3) can be solved by using the block coordinate descent (BCD) method to cyclically optimize the variables $\mathbf{w}_2$, $\boldsymbol{\theta}_k$, α_k and β_k, which is a three-step process.

Step 1) With $\mathbf{w}_2$ and $\boldsymbol{\theta}_k$ given, we separately take the derivative of them to find the optimal α_k° and β_k°. Mathematically, let

$$\frac{\partial f(\mathbf{w}_2,\boldsymbol{\theta}_k,\alpha_k,\beta_k)}{\partial\alpha_k}=0, \tag{20}$$

$$\frac{\partial f(\mathbf{w}_2,\boldsymbol{\theta}_k,\alpha_k,\beta_k)}{\partial\beta_k}=0. \tag{21}$$

Then, it is deduced that

$$\alpha_k^\circ=\frac{\zeta_k^2+\zeta_k\sqrt{\zeta_k^2+4}}{2}, \tag{22}$$

$$\zeta_k=\mathrm{Re}\{\beta_k^*\mathbf{w}_2^H\boldsymbol{\Phi}_k^H\boldsymbol{\theta}_k\}, \tag{23}$$

$$\beta_k^\circ=\frac{\sqrt{1+\alpha_k^\circ}\mathbf{w}_2^H\boldsymbol{\Phi}_k^H\boldsymbol{\theta}_k}{|\mathbf{h}_k^H\mathbf{w}_2|^2+\sum_{i=1}^{K}|\mathbf{w}_2^H\boldsymbol{\Phi}_k^H\boldsymbol{\theta}_i|^2+\sigma_k^2/P}, \tag{24}$$

where $\mathbf{w}_2$ and $\boldsymbol{\theta}_k$ denote the temporal optimization results in the last cyclical iteration, respectively. According to [37], [38], α_k can be also updated using the SINR $\gamma_{k,2}$.

Step 2) With $\boldsymbol{\theta}_k$, α_k and β_k given, the objective function of the problem (P3) can be simplified as

$$\max_{\mathbf{w}_2} \quad f(\mathbf{w}_2,\boldsymbol{\theta}_k,\alpha_k,\beta_k) \tag{25a}$$

$$\begin{aligned}
\Longleftrightarrow&\max_{\mathbf{w}_2}\sum_{k=1}^{K}\Bigg[2\sqrt{1+\alpha_k}\mathrm{Re}\{\beta_k^*\mathbf{w}_2^H\boldsymbol{\Phi}_k^H\boldsymbol{\theta}_k\}\\
&\qquad-|\beta_k|^2\left(|\mathbf{h}_k^H\mathbf{w}_2|^2+\sum_{i=1}^{K}|\mathbf{w}_2^H\boldsymbol{\Phi}_k^H\boldsymbol{\theta}_i|^2\right)\Bigg]
\end{aligned} \tag{25b}$$

$$\Longleftrightarrow\min_{\mathbf{w}_2} \quad \mathbf{w}_2^H\mathbf{U}\mathbf{w}_2-2\mathrm{Re}\{\mathbf{w}_2^H\mathbf{v}\}, \tag{25c}$$

where $\mathbf{U}=\sum_{k=1}^{K}|\beta_k|^2\left(\mathbf{h}_k\mathbf{h}_k^H+\sum_{i=1}^{K}\boldsymbol{\Phi}_k^H\boldsymbol{\theta}_i\boldsymbol{\theta}_i^H\boldsymbol{\Phi}_k\right)$ and $\mathbf{v}=\sum_{k=1}^{K}\sqrt{1+\alpha_k}\beta_k^*\boldsymbol{\Phi}_k^H\boldsymbol{\theta}_k$. Based on this, the problem (P3) is reformulated as

$$\min_{\mathbf{w}_2} \quad \mathbf{w}_2^H\mathbf{U}\mathbf{w}_2-2\mathrm{Re}\{\mathbf{w}_2^H\mathbf{v}\} \tag{26a}$$

$$s.t. \quad \mathrm{Tr}(\mathbf{w}_2\mathbf{w}_2^H)\leq 1. \tag{26b}$$

The Lagrangian associated with this problem is given by

$$\mathcal{L}(\mathbf{w}_2,\eta)=\mathbf{w}_2^H\mathbf{U}\mathbf{w}_2-2\mathrm{Re}\{\mathbf{w}_2^H\mathbf{v}\}+\eta\left(\mathbf{w}_2^H\mathbf{I}\mathbf{w}_2-1\right) \tag{27}$$

where η represents the Lagrange multiplier associated with the constraint. By setting $\frac{\partial\mathcal{L}(\mathbf{w}_2,\eta)}{\partial\mathbf{w}_2}=0$, we can obtain the optimal $\mathbf{w}_2^\circ$, which is given by

$$\mathbf{w}_2^\circ=\left(\eta\mathbf{I}+\mathbf{U}\right)^{-1}\mathbf{v}, \tag{28}$$

$$\eta^\circ=\min\left\{\eta\geq 0:\mathbf{w}_2^H\mathbf{I}\mathbf{w}_2\leq 1\right\}. \tag{29}$$

Step 3) With $\mathbf{w}_2$, α_k and β_k given, the objective function of the problem (P3) can be simplified as

$$\max_{\boldsymbol{\theta}_k} \quad f(\mathbf{w}_2,\boldsymbol{\theta}_k,\alpha_k,\beta_k) \tag{30a}$$

$$\Longleftrightarrow\max_{\boldsymbol{\theta}_k}\sum_{k=1}^{K}\Big[2\sqrt{1+\alpha_k}\mathrm{Re}\{\beta_k^*\mathbf{w}_2^H\boldsymbol{\Phi}_k^H\boldsymbol{\theta}_k\} \tag{30b}$$

$$-|\beta_k|^2\sum_{i=1}^{K}|\mathbf{w}_2^H\boldsymbol{\Phi}_k^H\boldsymbol{\theta}_i|^2\Big]. \tag{30c}$$

Based on the theory of quadratical constraint quadratic programming (QCQP), we have

$$\begin{aligned}
2\mathrm{Re}\{\beta_k^*\mathbf{w}_2^H\boldsymbol{\Phi}_k^H\boldsymbol{\theta}_k\}&=\beta_k^*\mathbf{w}_2^H\boldsymbol{\Phi}_k^H\boldsymbol{\theta}_k+\beta_k\boldsymbol{\theta}_k^H\boldsymbol{\Phi}_k\mathbf{w}_2,\\
&\triangleq\hat{\boldsymbol{\theta}}_k^H\mathbf{R}_k\hat{\boldsymbol{\theta}}_k=\mathrm{Tr}(\mathbf{R}_k\hat{\boldsymbol{\Theta}}_k),
\end{aligned} \tag{31}$$

$$|\mathbf{w}_2^H\boldsymbol{\Phi}_k^H\boldsymbol{\theta}_i|^2=\mathrm{Tr}\left(\mathbf{W}_2\boldsymbol{\Phi}_k^H\boldsymbol{\Theta}_i\boldsymbol{\Phi}_k\right), \tag{32}$$

where $\mathbf{W}_2\triangleq\mathbf{w}_2\mathbf{w}_2^H$, $\boldsymbol{\Theta}_i\triangleq\boldsymbol{\theta}_i\boldsymbol{\theta}_i^H$ and $\hat{\boldsymbol{\Theta}}_i\triangleq\hat{\boldsymbol{\theta}}_i\hat{\boldsymbol{\theta}}_i^H$

$$\mathbf{R}_k=\begin{bmatrix}\mathbf{0} & \beta_k\boldsymbol{\Phi}_k\mathbf{w}_2\\ \beta_k^*\mathbf{w}_2^H\boldsymbol{\Phi}_k^H & \mathbf{0}\end{bmatrix}, \tag{33}$$

$$\hat{\boldsymbol{\theta}}_k=\begin{bmatrix}\boldsymbol{\theta}_k\\ 1\end{bmatrix}. \tag{34}$$

Based on this, the problem (P3) is reformulated as

$$\text{(P4)} \quad \max_{\hat{\boldsymbol{\Theta}}_k} \quad \sum_{k=1}^{K}\Big[\sqrt{1+\alpha_k}\mathrm{Tr}(\mathbf{R}_k\hat{\boldsymbol{\Theta}}_k)$$

$$- |\beta_k|^2 \sum_{i=1}^{K} \mathrm{Tr}\left(\mathbf{W}_2 \mathbf{\Phi}_k^H \mathbf{\Theta}_i \mathbf{\Phi}_k\right)\Big], \quad (35a)$$

$$s.t. \quad \left[\sum_{k=1}^{K} \hat{\mathbf{\Theta}}_k\right]_{l,l} \leq 1, \forall l \in \mathcal{L}, \quad (35b)$$

$$\left[\hat{\mathbf{\Theta}}_k\right]_{L+1,L+1} = 1, \forall k \in \mathcal{K}, \quad (35c)$$

$$\hat{\mathbf{\Theta}}_k \succeq \mathbf{0}, \ \mathrm{rank}\left(\hat{\mathbf{\Theta}}_k\right) = 1, \forall k \in \mathcal{K}. \quad (35d)$$

Dropping the constraint $\mathrm{rank}\left(\hat{\mathbf{\Theta}}_k\right) = 1$, this optimization problem is convex over $\hat{\mathbf{\Theta}}_k$ and can be easily solved by the CVX solver. Based on its optimal solution $\hat{\mathbf{\Theta}}_k^{\circ}$, singular value decomposition or the Gaussian randomization method can be employed to recover the rank-one solution $\boldsymbol{\theta}_k^{\circ}$.

C. Optimization of Parameters T_1, T_2 and T_c

Once $\mathbf{w}_1$, $\mathbf{w}_2$ and $\boldsymbol{\theta}_k$ are obtained, the problem (P1) becomes more tractable. Since T_1 can be computed via $T_1 = T - T_2$, the problem (P1) is firstly rewritten as

$$(\mathrm{P5}) \quad \max_{T_2, T_c} \quad T_2 W \sum_{k=1}^{K} \log\left(1 + \gamma_{k,2}\right) + \frac{T_c f_c}{C_c}, \quad (36a)$$

$$s.t. \quad \left(\chi P \|\mathbf{H}\mathbf{w}_1\|^2 + L\mu\right) T_2 + \varepsilon_c f_c^3 T_c \leq \chi T P \|\mathbf{H}\mathbf{w}_1\|^2, \quad (36b)$$

$$0 \leq T_2 \leq T, 0 \leq T_c \leq T. \quad (36c)$$

It can be clearly observed that (P5) is a linear programming problem, thus it can be easily solved. Up to this point, the problem (P1) is thoroughly solved.

D. Complexity Analysis

Maximization of sum computational bits in this section corresponds to the aforementioned three optimization problems. For the problem (P1), it is decomposed into three tractable optimization problems (P2), (P3) and (P5). Compared to the problems (P2) and (P5), the problem (P3) has the highest complexity. For the problem (P3), it can be solved by a three-step iteration process, in which the subproblem (P4) dominates its complexity. When the interior-point method (IPM) is employed, the complexity of the subproblem (P4) is given by [39]

$$C_{\mathrm{P4}} = \frac{1}{\varepsilon}\sqrt{2K(N+1) + 2(K+L)}\big[8nK(N+1)^3 + 4n^2K(N+1)^2 + (4n^2+8n)(K+L)\big], \quad (37)$$

where $n = \mathcal{O}\{K(L+1)^2\}$. ε denotes the iteration accuracy. From multiple observations, we find the iteration number of the three-step process is often small. Assuming that the iteration number is T_{ite}, the complexity of the problem (P1) is approximately given by $C_{\mathrm{P1}} = T_{\mathrm{ite}} C_{\mathrm{P4}}$.

IV. Rate Maximization of Sum Computational Bits Using Element Clustering

As the element number of IRS rises sharply, the control and computing complexity for individually adjusting each of them goes up rapidly. Different from Section III-B, this section will employ element clustering to realize BackCom, which provides a manageable way for the IRS comprising a large number of elements. In this paper, element clustering complies with the following simple principle: an IRS is divided into K clusters equally and each element cluster can work like an equivalent big element.

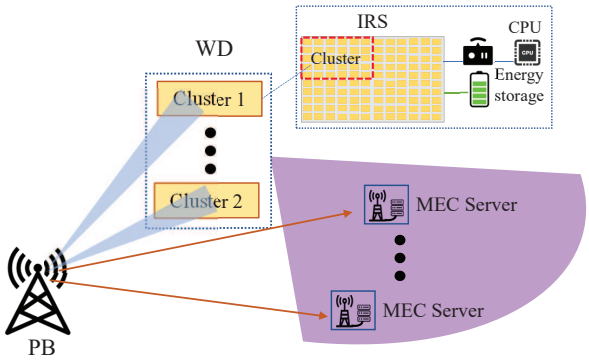

Fig. 2. IRS-based backscatter communication based on element clustering.

Specifically, an IRS is divided into K clusters equally, with each cluster having L/K elements, as shown in Fig. 2. The cascaded channel from the PB to the k-th MEC server through the i-th element cluster is modeled as $\mathbf{f}_{k,i}^H \mathbf{\Theta}_i \mathbf{H}_i = \boldsymbol{\theta}_i^H \mathrm{diag}\{\mathbf{f}_{k,i}^H\}\mathbf{H}_i$, $k \in \mathcal{K}$, $i \in \mathcal{K}$, where $\mathbf{f}_{k,i} \in \mathbb{C}^{L/K \times 1}$ and $\mathbf{H}_i \in \mathbb{C}^{L/K \times N}$ denote the channel gains from the i-th element cluster to the k-th MEC server and from the PB to the i-th element cluster, respectively. $\mathbf{\Theta}_i$ and $\boldsymbol{\theta}_i$ represent the diagonal reflection-coefficient matrix and the reflection-coefficient vector of the i-th element cluster, respectively. Based on element clusters, the received signal at the k-th MEC server is given by (38) at the bottom of next page. In the following, we will discuss two cluster operation modes according to different operating mechanisms.

A. Independent Cluster Operation Mode

This subsection considers the independent cluster operation mode for the sake of easy control, in which each cluster serves a single-antenna MEC server. In other words, the data offloading task is divided into K parts, each of which is assigned to one element cluster. Each element cluster sends the respective subtask to the corresponding MEC server via BackCom independently. Thus, the received signal at the k-th MEC server is given by

$$y_{k,2} = \sqrt{P}\left[\theta_1 x_1, \theta_2 x_2, \cdots, \theta_K x_K\right] \begin{bmatrix} \tilde{\boldsymbol{\theta}}_1^H \mathrm{diag}\{\mathbf{f}_{k,1}^H\}\mathbf{H}_1 \\ \tilde{\boldsymbol{\theta}}_2^H \mathrm{diag}\{\mathbf{f}_{k,2}^H\}\mathbf{H}_2 \\ \vdots \\ \tilde{\boldsymbol{\theta}}_K^H \mathrm{diag}\{\mathbf{f}_{k,K}^H\}\mathbf{H}_K \end{bmatrix} \mathbf{w}_2 + \sqrt{P}\mathbf{h}_k^H \mathbf{w}_2 s + n_k. \quad (39)$$

where θ_i is related to the power reflection ratio P_i of all elements at the i-th cluster with $\theta_i = \sqrt{P_i}$. Clearly, the power reflection ratio of all elements for each cluster is set as the same value. $\tilde{\boldsymbol{\theta}}_i$ is a unit complex vector and used to offset the phase of $\mathrm{diag}\{\mathbf{f}_{k,i}^H\}\mathbf{H}_i\mathbf{w}_2$. It is not difficult to find that each cluster can be viewed as an equivalent element which can receive and forward more power. Moreover, the power

reflection ratio P_i is able to control the reflection power.

Let $\mathbf{h}_{k,i} = \sqrt{P_i}\tilde{\boldsymbol{\theta}}_i^H \text{diag}\{\mathbf{f}_{k,i}^H\}\mathbf{H}_i$. The SINR at the k-th MEC server is given by

$$\gamma_{k,2} = \frac{|\mathbf{h}_{k,k}\mathbf{w}_2|^2}{|\mathbf{h}_k^H\mathbf{w}_2|^2 + \sum_{i=1,i\neq k}^K |\mathbf{h}_{k,i}\mathbf{w}_2|^2 + \sigma_k^2/P}. \tag{40}$$

Then, the rate maximization problem of IRS-BackCom using element cluster in the independent cluster operation mode can be formulated as

$$\max_{\mathbf{w}_2,P_i} \quad \sum_{k=1}^K \log\left(1+\gamma_{k,2}\right), \tag{41a}$$
$$s.t. \quad \text{Tr}(\mathbf{w}_2\mathbf{w}_2^H) \leq 1, \tag{41b}$$
$$0 \leq P_i \leq 1,\ i \in \mathcal{K}. \tag{41c}$$

To make this non-convex optimization problem tractable, the Lagrangian dual transform and the quadratic transform [36] are employed to reformulate the objective function as

$$f(\mathbf{w}_2,P_i,\alpha_k,\beta_k) = \sum_{k=1}^K \log\left(1+\alpha_k\right) - \alpha_k + \sum_{k=1}^K 2\sqrt{1+\alpha_k}\text{Re}\{\beta_k^*\text{A}_k\} - \sum_{k=1}^K |\beta_k|^2\text{B}_k, \tag{42}$$

where

$$\text{A}_k = \mathbf{h}_{k,k}\mathbf{w}_2 = \sqrt{P_k}\tilde{\boldsymbol{\theta}}_k^H\text{diag}\{\mathbf{f}_{k,k}^H\}\mathbf{H}_k\mathbf{w}_2, \tag{43}$$

$$\begin{aligned}\text{B}_k &= |\mathbf{h}_k^H\mathbf{w}_2|^2 + \sum_{i=1}^K |\mathbf{h}_{k,i}\mathbf{w}_2|^2 + \sigma_k^2/P \\ &= |\mathbf{h}_k^H\mathbf{w}_2|^2 + \sum_{i=1}^K P_i|\tilde{\boldsymbol{\theta}}_i^H\text{diag}\{\mathbf{f}_{k,i}^H\}\mathbf{H}_i\mathbf{w}_2|^2 + \sigma_k^2/P.\end{aligned} \tag{44}$$

Therefore, the optimization problem is rewritten as

$$\text{(P6)} \quad \max_{\mathbf{w}_2,P_i} \quad \sum_{k=1}^K f(\mathbf{w}_2,P_i,\alpha_k,\beta_k), \tag{45a}$$
$$s.t. \quad \text{Tr}(\mathbf{w}_2\mathbf{w}_2^H) \leq 1, \tag{45b}$$
$$0 \leq P_i \leq 1,\ i \in \mathcal{K}. \tag{45c}$$

Similar to the problem (P3), the problem (P6) can also be solved by invoking a three-step process to cyclically optimize the variables $\mathbf{w}_2$, P_i, α_k and β_k.

Step 1) When $\mathbf{w}_2$ and $\boldsymbol{\theta}_k$ are given, the optimal α_k° and β_k° are given by

$$\alpha_k^\circ = \gamma_{k,2}, \tag{46}$$
$$\beta_k^\circ = \frac{\sqrt{1+\alpha_k^\circ}\text{A}_k}{\text{B}_k}. \tag{47}$$

Step 2) When α_k, β_k and P_i are fixed, the optimization problem (P6) can be solved similar to **Step 2**) in Section III-B. Specifically, define $\mathbf{g}_{k,i}^H = \sqrt{P_i}\tilde{\boldsymbol{\theta}}_i^H\text{diag}\{\mathbf{f}_{k,i}^H\}\mathbf{H}_i$, $\mathbf{U} = \sum_{k=1}^K |\beta_k|^2\left(\mathbf{h}_k\mathbf{h}_k^H + \sum_{i=1}^K \mathbf{g}_{k,i}\mathbf{g}_{k,i}^H\right)$, and $\mathbf{v} = \sum_{k=1}^K \sqrt{1+\alpha_k}\beta_k\mathbf{g}_{k,k}$. Note that $\sqrt{P_i}$ and $\tilde{\boldsymbol{\theta}}_i$ denote the temporal optimization results in the last iteration. Then, the objective function is further expressed as

$$\max_{\mathbf{w}_2} \quad f(\mathbf{w}_2,P_i,\alpha_k,\beta_k) \Longleftrightarrow \min_{\mathbf{w}_2} \quad \mathbf{w}_2^H\mathbf{U}\mathbf{w}_2 - 2\text{Re}\{\mathbf{w}_2^H\mathbf{v}\}, \tag{48}$$

The Lagrangian associated with this problem is given by

$$\mathcal{L}(\mathbf{w}_2,\eta) = \mathbf{w}_2^H\mathbf{U}\mathbf{w}_2 - 2\text{Re}\{\mathbf{w}_2^H\mathbf{v}\} + \eta\left(\mathbf{w}_2^H\mathbf{I}\mathbf{w}_2 - 1\right), \tag{49}$$

where η represents the Lagrange multiplier associated with the constraint. By setting $\frac{\partial\mathcal{L}(\mathbf{w}_2,\eta)}{\partial\mathbf{w}_2} = 0$, we can obtain the optimal $\mathbf{w}_2^\circ$, which is given by

$$\mathbf{w}_2^\circ = \left(\eta\mathbf{I}+\mathbf{U}\right)^{-1}\mathbf{v}, \tag{50}$$
$$\eta^\circ = \min\left\{\eta \geq 0 : \mathbf{w}_2^H\mathbf{I}\mathbf{w}_2 \leq 1\right\}. \tag{51}$$

Step 3) When α_k, β_k and $\mathbf{w}_2$ are fixed, the problem (P6) is simplified as

$$\text{(P7)} \quad \max_{P_i} \quad \sum_{k=1}^K \Bigg[2\sqrt{1+\alpha_k}\text{Re}\{\sqrt{P_k}\beta_k^*\tilde{\boldsymbol{\theta}}_k^H\text{diag}\{\mathbf{f}_{k,k}^H\}\mathbf{H}_k\mathbf{w}_2\} - |\beta_k|^2\sum_{i=1}^K P_i|\tilde{\boldsymbol{\theta}}_i^H\text{diag}\{\mathbf{f}_{k,i}^H\}\mathbf{H}_i\mathbf{w}_2|^2\Bigg], \tag{52a}$$
$$s.t. \quad 0 \leq P_i \leq 1,\ i \in \mathcal{K}. \tag{52b}$$

Clearly, this problem is convex and easily solved.

B. Joint Cluster Operation Mode

This subsection considers the joint cluster operation mode, in which the K element clusters collaborate to serve K single-antenna MEC servers. In other words, the K element clusters are regarded as K equivalent elements, which are able to achieve joint passive beamforming to send K subtasks to the K MEC servers via BackCom. Thus, the received signal at

$$y_{k,2} = \sqrt{P}\left[\mathbf{f}_{k,1}^H,\mathbf{f}_{k,2}^H,\ldots,\mathbf{f}_{k,K}^H\right]\begin{bmatrix}\boldsymbol{\Theta}_1 & \mathbf{0} & \mathbf{0} & \mathbf{0}\\ \mathbf{0} & \boldsymbol{\Theta}_2 & \mathbf{0} & \mathbf{0}\\ \mathbf{0} & \mathbf{0} & \ddots & \mathbf{0}\\ \mathbf{0} & \mathbf{0} & \mathbf{0} & \boldsymbol{\Theta}_K\end{bmatrix}\begin{bmatrix}\mathbf{H}_1\\ \mathbf{H}_2\\ \vdots\\ \mathbf{H}_K\end{bmatrix}\mathbf{w}_2 s + \sqrt{P}\mathbf{h}_k^H\mathbf{w}_2 s + n_k =$$

$$\sqrt{P}\left[\boldsymbol{\theta}_1^H,\boldsymbol{\theta}_2^H,\cdots,\boldsymbol{\theta}_K^H\right]\begin{bmatrix}\text{diag}\{\mathbf{f}_{k,1}^H\}\mathbf{H}_1\\ \text{diag}\{\mathbf{f}_{k,2}^H\}\mathbf{H}_2\\ \vdots\\ \text{diag}\{\mathbf{f}_{k,K}^H\}\mathbf{H}_K\end{bmatrix}\mathbf{w}_2 s + \sqrt{P}\mathbf{h}_k^H\mathbf{w}_2 s + n_k = \sqrt{P}\sum_{i=1}^K \boldsymbol{\theta}_i^H\text{diag}\{\mathbf{f}_{k,i}^H\}\mathbf{H}_i\mathbf{w}_2 s + \sqrt{P}\mathbf{h}_k^H\mathbf{w}_2 s + n_k. \tag{38}$$

TABLE I
SIMULATION PARAMETERS.

Parameter	Value
Rician factor from PB to IRS or MEC servers κ_1	2
Rician factor from IRS to MEC servers κ_2	3
Distance from PB to IRS d_{pi}	60 m
Element number of IRS L	64
Average distance from PB to MEC servers d_{pm}	65 m
Antenna number of PB	4
Antenna gain of the PB	30dBi
Transmit power of the PB P	6 dBW
Power of all noise σ^2	10^{-8} W
Communication bandwidth W	10^6 Hz
Energy harvesting efficiency of IRS χ	0.8
Local computing frequency of the CPU f_{c}	5×10^8 Hz
Required number of CPU cycles C_{c}	100
Energy consumption coefficient of processor's chip ε_{c}	10^{-26}
Time block T	0.1 s
Number of active antennas replacing IRS N_{a}	2 or 4
Power of active antennas replacing IRS P_{a}	18 dBm or 9 dBm

the k-th MEC server is given by

$$y_{k,2} = \sqrt{P}\mathbf{m}^H s\$_k\mathbf{w}_2 + \sqrt{P}\mathbf{h}_k^H\mathbf{w}_2 s + n_k$$
$$= \sqrt{P}\left(\sum_{i=1}^{K}\mathbf{m}_i^H x_i\right)\$_k\mathbf{w}_2 + \sqrt{P}\mathbf{h}_k^H\mathbf{w}_2 s + n_k, \quad (53)$$

where

$$\$_k = \begin{bmatrix} \tilde{\boldsymbol{\theta}}_1^H \text{diag}\{\mathbf{f}_{k,1}^H\}\mathbf{H}_1 \\ \tilde{\boldsymbol{\theta}}_2^H \text{diag}\{\mathbf{f}_{k,2}^H\}\mathbf{H}_2 \\ \vdots \\ \tilde{\boldsymbol{\theta}}_K^H \text{diag}\{\mathbf{f}_{k,K}^H\}\mathbf{H}_K \end{bmatrix}. \quad (54)$$

For the sake of easy control, $\tilde{\boldsymbol{\theta}}_1$ can be set as a unit random complex vector, such as $\mathbf{1}$. It is not difficult to observe that (53) has a similar form to (4). Clearly, the rate maximization problem of IRS-BackCom in the joint cluster operation mode can be solved using the same method as Section III-B, and thus we don't repeat here.

C. Complexity analysis

The problem (P6) is solved by three steps. The complexity of the first step is given by $\mathcal{O}\{2KNL\}$. The second step involves the matrix inverse operation and the bisection method, thus its complexity is determined by $\mathcal{O}\{N^3\log_2(\eta_{\max}-\eta_{\min})\}$. Using the IPM method, the complexity of the third step is approximately given by $\mathcal{O}\{K^3+2KNL\}$. Assuming that the iteration number is T_{ite}, the complexity of the problem (P1) in the independent cluster operation mode is approximately given by $C_{\text{independent}} = T_{\text{ite}}\mathcal{O}\{N^3\log_2(\eta_{\max}-\eta_{\min})+K^3+4KNL)\}$. For joint cluster operation mode, it is performed similar to Section III-B with lower complexity, which is given by

$$C_{\text{joint}} = \frac{T_{\text{ite}}}{\varepsilon}\sqrt{2K(N+1)+4K}\big[8nK(N+1)^3 + 4n^2K(N+1)^2 + 8(n^2+2n)K\big], \quad (55)$$

where $n = \mathcal{O}\{K(K+1)^2\}$.

V. SIMULATION RESULTS

In this section, numerical simulations will be conducted to show the communication performance of wireless powered MEC assisted by IRS-BackCom. In simulations, it is assumed that all involved channels are slowly fading, while all channel gains remain unchanged in a time block and obey Rician distribution across a great many blocks. All involved path losses are given by PL = $\text{PL}_0 - 25\lg(d/d_0)$ dB, where PL_0 = -30 dB represents the path loss at d_0, d is the transmission distance and d_0 = 1m denotes the reference distance. Moreover, the Rician factors from the PB to the IRS and from the PB to the MEC servers are denoted by κ_1, while those from the IRS to the MEC servers are given by κ_2. Since BackCom occurs only in the front half-sphere of the IRS, an additional 3 dBi gain needs to be considered for each element. Assuming that the directional antenna is employed at the PB, there exists an antenna gain of 30 dBi from the PB to the IRS. Note that the proposed strategy and scheme in this paper are also suitable to other channel models.

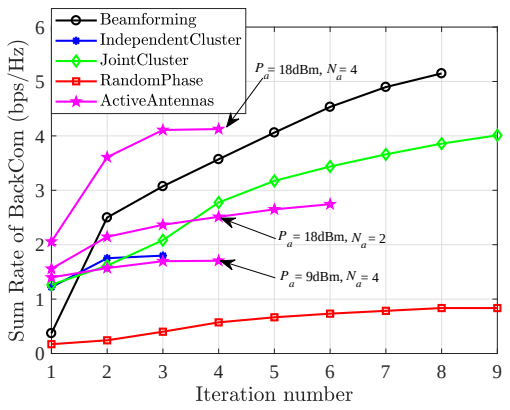

Fig. 3. Convergence behavior of using the three-step process to maximize the sum rate of IRS-BackCom in a random observation.

This section will present the proposed three schemes and two counterparts. For convenience, they are represented by some simple legends as follows.

- *Beamforming*: Each element of IRS is individually controlled to realize wireless powered MEC assisted by IRS-BackCom, as detailed in Section II and III.
- *IndependentCluster*: Element clustering of IRS is employed, where one cluster serves a single-antenna MEC server, as detailed in Section IV-A.
- *JointCluster*: Element clustering of IRS is employed, where element clusters collaborate to serve K single-antenna MEC servers, as detailed in Section IV-B.
- *ActiveAntennas*: Using an active transmitter to offload computational bits instead of IRS-BackCom. The transmitter has the same position as the IRS, and its transmit power and antenna number are P_a and N_a, respectively.
- *RandomPhase*: The phase of each element at the IRS is generated randomly and the amplitude is set as one to realize wireless powered MEC assisted by IRS-BackCom.

TABLE I lists some important parameters. When some parameters are investigated in the following simulation figures, they are variables rather than the values given in TABLE I. Since multiple MEC servers are involved, the distances from the PB to them are generated from the interval [d_{pm}-10, d_{pm}+10] randomly and uniformly, while those from the

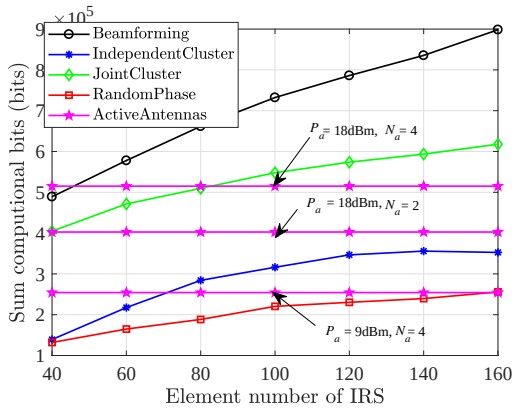

Fig. 4. The relationship between the sum computational bits $R_{\rm b}+R_{\rm c}$ of system and the element number L of IRS.

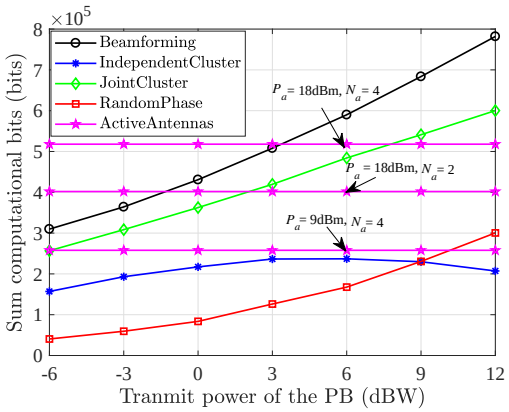

Fig. 6. The relationship between the sum computational bits $R_{\rm b}+R_{\rm c}$ of system and the transmit power P of the PB.

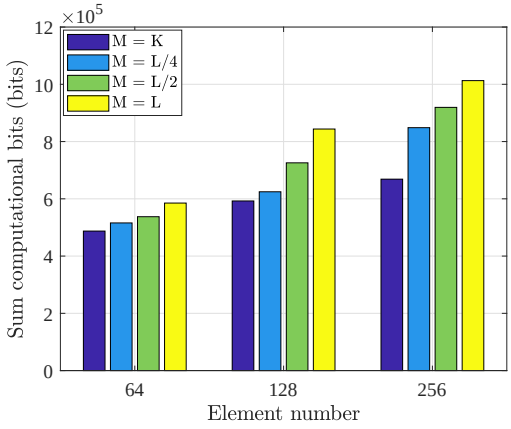

Fig. 5. The effect of element cluster number M of IRS on the sum computational bits $R_{\rm b}+R_{\rm c}$ of system.

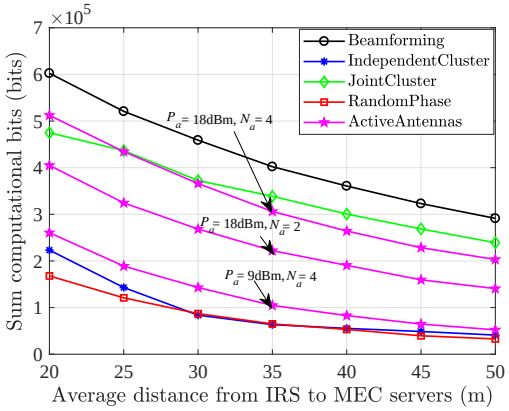

Fig. 7. The relationship between the sum computational bits $R_{\rm b}+R_{\rm c}$ of system and the average distance $d_{\rm im}$ from the IRS to the MEC servers.

IRS to them are taken from the interval [$d_{\rm im}$-10, $d_{\rm im}$+10].

In Section III-B, the three-step process is employed to maximize the sum rate of IRS-BackCom $R_{\rm sum} = \sum_{k=1}^{K}\log\left(1+\gamma_{k,2}\right)$. Fig. 3 presents the sum rate $R_{\rm sum}$ in terms of the iteration number $T_{\rm ite}$ in a random observation. From Fig. 3, we observe that all curves converge very quickly. From many observations, we also find that the scheme of *IndependentCluster* does not always have a good convergence. In this case, the best result in the iterative process (the maximum number of iteration is set as 100) is used as a suboptimal solution.

Fig. 4 plots how the sum computational bits $R_{\rm b}+R_{\rm c}$ of system depends on the element number L of IRS. From Fig. 4, it is clearly seen that the sum computational bits grow up with the elements of IRS increasing expect for the scheme of *ActiveAntennas*. The reason is that an increase in the elements of IRS is beneficial to harvesting or reflecting more power of wireless signal from the PB. However, the rate of growth tends to slow down as the element number becomes large. There are two possible reasons: i) The energy consumption $T_2L\mu$ at IRS is a function of the element number; ii) The data offloading rate is a sum of logarithm functions of the SINRs at MEC servers, which have a positive relation with the element number of IRS.

Additionally, from Fig. 4 we observe that the scheme of *Beamforming* yields the best performance, followed by *JointCluster*, *IndependentCluster* and *RandomPhase* in all the BackCom schemes. That is primarily because more elements are individually optimized to suppress co-channel interference. Compared to *ActiveAntennas*, the BackCom schemes may achieve a comparable or better communication performance with the given transmit power and antenna number. This result indicates IRS-BackCom can substitute the active transmission to a certain extent. Fig. 5 depicts how the element cluster number M affects the sum computational bits $R_{\rm b}+R_{\rm c}$ of system in the scheme of *JointCluster*. From Fig. 5, it is not difficult to find that an increase in M contributes to improving $R_{\rm b}+R_{\rm c}$. The reason is that the elements of IRS are regulated more critically.

Fig. 6 and Fig. 7 show how the sum computational bits $R_{\rm b}+R_{\rm c}$ of system is affected by the transmit power P of the PB and the average distance $d_{\rm im}$ from the IRS to the MEC servers, respectively. From the two figures, we observe that $R_{\rm b}+R_{\rm c}$ grows up when P becomes higher. However, the growth rate is slowing down. On the contrary, as $d_{\rm im}$ increases, $R_{\rm b}+R_{\rm c}$ decreases but the rate of descent slows down gradually. The reason of these results in the final analysis is that the received power at the MEC servers is reduced.

Fig. 8 presents the relationship between the sum computational bits $R_{\rm b}+R_{\rm c}$ and the number K of MEC servers.

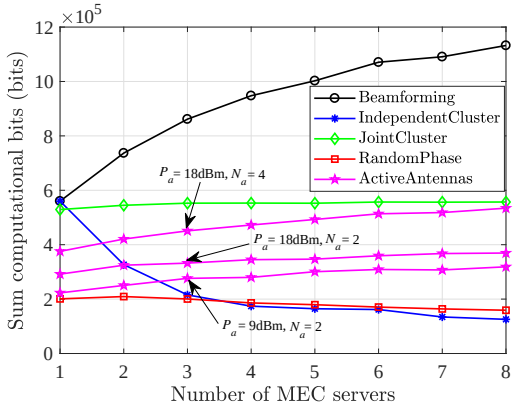

Fig. 8. The relationship between the sum computational bits $R_{\rm b} + R_{\rm c}$ of system and the number of the MEC servers.

Note that here the element number of IRS is set as $L = K \times floor(100/K)$, where $floor(x)$ is a function of x and rounds x to the nearest integer less than or equal to it. It is not difficult to find that the sum computational bits go up with the number of MEC servers for the schemes of *Beamforming*, *ActiveAntennas* and *JointCluster*, while the schemes of *RandomPhase* and *IndependentCluster* have exactly the reverse results. These results indicate the communication performance can be improved if the degree of user freedom is deeply exploited. On the contrary, spatial multiplexing may result in stronger mutual interference if the transmitter and receivers are not well coordinated.

VI. Conclusions and Future Works

This paper proposed to apply IRS-BackCom in the MEC network and then maximized sum computational bits. By jointly optimizing the beamforming vector at the PB, the backscatter matrix at the IRS, the time scheduling of two-phase process, as well as the time of local computing, sum computational bits were maximized. In addition, element clustering was proposed to realize BackCom with two cluster operation modes presented, namely independent cluster operation mode and joint cluster operation mode. According to numerical results, it can be concluded that: 1) As an alternative to active antennas, IRS can be leveraged for EH and BackCom, achieving computational data offloading in a self-sustainable wireless powered manner; 2) The achievable performance by the scheme of *Beamforming* is superior to *JointCluster* *RandomPhase* and *IndependentCluster*, but the complexity of *Beamforming* is the highest; 3) The sum computational bits are improved, when the element number and the transmit power increase or the average distance from the IRS to the MEC servers shortens; 4) The sum computational bits go up with the number of MEC servers for the schemes of *Beamforming*, *ActiveAntennas* and *JointCluster*, while the schemes of *RandomPhase* and *IndependentCluster* have exactly the reverse results.

Based on this work, several research agendas worthy of further investigation are as follows. 1) Considering that channel estimation is extremely important, it is necessary to investigate how to estimate channel information accurately and quickly for the scenario of IRS-BackCom in more depth; 2) Considering that the computational complexity of the proposed optimization scheme is high, it is of significance to design an efficient algorithm; 3) In addition to the partial offloading strategy in this paper, the binary offloading strategy needs to be studied; 4) How to apply IRS to multi-tier computing systems is a promising research direction.

References

[1] Y. Mao, C. You, J. Zhang, K. Huang, and K. B. Letaief, "A survey on mobile edge computing: The communication perspective," *IEEE Commun. Surveys Tuts.*, vol. 19, no. 4, pp. 2322-2358, 4th Quart., 2017.

[2] P. X. Nguyen, D. H. Tran, O. Onireti, P. T. Tin, S. Q. Nguyen, S. Chatzinotas, and H. V. Poor, "Backscatter-assisted data offloading in OFDMA-based wireless-powered mobile edge computing for IoT networks," *IEEE Internet Things J.*, vol. 8, no. 11, pp. 9233-9243, Jun. 2021.

[3] P. Mach, and Z. Becvar, "Mobile edge computing: A survey on architecture and computation offloading," *IEEE Commun. Surveys Tuts.*, vol. 19, no. 3, pp. 1628-1656, 3rd Quart., 2017.

[4] F. Zhou, and R. Q. Hu, "Computation efficiency maximization in wireless-powered mobile edge computing networks," *IEEE Trans. Wireless Commun.*, vol. 19, no. 5, pp. 3170-3184, May 2020.

[5] L. Shi, Y. Ye, G. Zheng and G. Lu, "Computational EE fairness in backscatter-assisted wireless powered MEC networks," *IEEE Wireless Commun. Lett.*, vol. 10, no. 5, pp. 1088-1092, May 2021.

[6] Y. Wu, Y. Wang, F. Zhou, and R. Q. Hu, "Computation efficiency maximization in OFDMA-based mobile edge computing networks," *IEEE Commun. Lett.*, vol. 24, no. 1, pp. 159-163, Jan. 2020

[7] D. Altinel, and G. K. Kurt, "Modeling of multiple energy sources for hybrid energy harvesting IoT systems," *IEEE Internet Things J.*, vol. 6, no. 6, pp. 10846-10854, Dec. 2019.

[8] W. Wang, J. Tang, N. Zhao, X. Liu, X. Y. Zhang, Y. Chen, and Y. Qian, "Joint precoding optimization for secure SWIPT in UAV-aided NOMA networks," *IEEE Trans. Commun.*, vol. 68, no. 8, pp. 5028-5040, Aug. 2020

[9] S. Bi, Y. Zeng, and R. Zhang, "Wireless powered communication networks: An overview," *IEEE Wireless Commun.*, vol. 23, no. 2, pp. 10-18, Apr. 2016.

[10] F. Wang, J. Xu, and S. Cui, "Optimal energy allocation and task offloading policy for wireless powered mobile edge computing systems," *IEEE Trans. Wireless Commun.*, vol. 19, no. 4, pp. 2443-2459, Apr. 2020.

[11] S. Bi, and Y. J. Zhang, "Computation rate maximization for wireless powered mobile-edge computing with binary computation offloading," *IEEE Trans. Wireless Commun.*, vol. 17, no. 6, pp. 4177-4190, Jun. 2018.

[12] G. Wang, F. Gao, R. Fan, and C. Tellambura, "Ambient backscatter communication systems: detection and performance analysis," *IEEE Trans. Commun.*, vol. 64, no. 11, pp. 4836-4846, Nov. 2016.

[13] S. Gong, Y. Xie, J. Xu, D. Niyato, and Y.-C. Liang, "Deep reinforcement learning for backscatter-aided data offloading in mobile edge computing," *IEEE Netw.*, vol. 34, no. 5, pp. 106-113, Sep./Oct. 2020

[14] Y. E. A. Zou, "Backscatter-aided hybrid data offloading for wireless powered edge sensor networks," in *Proc. IEEE Global Commun. Conf. (GLOBECOM)*, Waikoloa, HI, USA, Dec. 2019, pp. 1-6.

[15] Y. Ye, L. Shi, X. Chu, D. Li, and G. Lu, "Delay minimization in wireless powered mobile edge computing with hybrid BackCom and AT," *IEEE Wireless Commun. Lett.*, vol. 10, no. 7, pp. 1532-1536, Jul. 2021.

[16] Y. Xu, B. Gu, R. Q. Hu, D. Li, and H. Zhang, "Joint computation offloading and radio resource allocation in MEC-based wireless-powered backscatter communication networks," *IEEE Trans. Veh. Technol.*, vol. 70, no. 6, pp. 6200-6205, Jun. 2021.

[17] S. Gong, X. Lu, D. Hoang, D. Niyato, L. Shu, D. Kim, and Y. Liang, "Toward smart wireless communications via intelligent reflecting surfaces: A contemporary survey," *IEEE Commun. Surveys Tuts.*, vol. 22, no. 4, pp. 2283-2314, 4th Quart 2020.

[18] M. Di Renzo, A. Zappone, M. Debbah, Mo.-S. Alouini, C. Yuen, J. d. Rosny, and S. Tretyakov, "Smart radio environments empowered by reconfigurable intelligent surfaces: How it works, state of research, and the road ahead," *IEEE J. Sel. Areas Commun.*, vol. 38, no. 11, pp. 2450-2525, Nov. 2020.

[19] S. Xu, J. Liu, T. K. Rodrigues, and N. Kato, "Envisioning intelligent reflecting surface empowered space-air-ground integrated network," *IEEE Netw.*, vol. 35, no. 6, pp. 225-232, Nov./Dec. 2021.

[20] S. Xu, Y. Du, J. Liu, and J. Li, "Weighted sum rate maximization in IRS-BackCom enabled downlink multi-cell MISO network," *IEEE Commun. Lett.*, vol. 26, no. 3, pp. 642-646, Mar. 2022.

[21] L. Zhang, X. Cen, S. Liu, Q. Zhang, J. Zhao, J. Dai, G. Bai, X. Wan, Q. Cheng, G. Castaldi, G. Galdi, and T. Cui, "Space-time-coding digital metasurface," *Nat. Commun.*, vol. 9, no. 1, pp. 1-11, Oct. 2018.

[22] X. Zhou, S. Yan, Q. Wu, F. Shu, and D. W. K. Ng, "Intelligent reflecting surface (IRS)-aided covert wireless communications with delay constraint," 2020, *arXiv*: 2011.03726. [Online] Available: https://arxiv.org/abs/2011.03726

[23] C. Wu, S. Yan, X. Zhou, R. Chen, and J. Sun, "Intelligent reflecting surface (IRS)-aided covert communication with Warden's statistical CSI," *IEEE Wireless Commun. Lett.*, vol. 10, no. 7, pp. 1449-1453, Jul. 2021.

[24] S. Yan, X. Zhou, D. W. K. Ng, J. Yuan, N. Al-Dhahir, "Intelligent reflecting surface for wireless communication security and privacy," 2021, *arXiv*: 2103.16696. [Online] Available: https://arxiv.org/abs/2103.16696

[25] T. Bai, C. Pan, Y. Deng, M. Elkashlan, A. Nallanathan, and L. Hanzo, "Latency minimization for intelligent reflecting surface aided mobile edge computing," *IEEE J. Sel. Areas Commun.*, vol. 38, no. 11, pp. 2666-2682, Nov. 2020.

[26] T. Bai, C. Pan, H. Ren, Y. Deng, M. Elkashlan, and A. Nallanathan, "Resource allocation for intelligent reflecting surface aided wireless powered mobile edge computing in OFDM systems," *IEEE Trans. Wireless Commun.*, to be published, doi: 10.1109/TWC.2021.3067709.

[27] W. Yan, X. Yuan, and X. Kuai, "Passive beamforming and information transfer via large intelligent surface," *IEEE Wireless Commun. Lett.*, vol. 9, no. 4, pp. 533-537, Apr. 2020.

[28] W. Zhao, G. Wang, S. Atapattu, T. A. Tsiftsis, and C. Tellambura, "Is backscatter link stronger than direct link in reconfigurable intelligent surface-assisted system?" *IEEE Commun. Lett.*, vol. 24, no. 6, pp. 1342-1346, Jun. 2020.

[29] S. Xu, J. Liu, and J. Zhang, "Resisting undesired signal through IRS-based backscatter communication system," *IEEE Commu. Lett.*, vol. 25, no. 8, pp. 2743-2747, Aug. 2021.

[30] S. Xu, J. Liu, and Y. Cao, "Intelligent reflecting surface empowered physical layer security: signal cancellation or jamming?," *IEEE Internet Things J.*, vol. 9, no. 2, pp. 1265-1275, Jan. 2022.

[31] F. Wang, J. Xu, X. Wang, and S. Cui, "Joint offloading and computing optimization in wireless powered mobile-edge computing systems," *IEEE Trans. Wireless Commun.*, vol. 17, no. 3, pp. 1784-1797, Mar. 2018.

[32] D. Mishra, and G. C. Alexandropoulos, "Transmit precoding and receive power splitting for harvested power maximization in MIMO SWIPT systems," *IEEE Trans. Green Commun. Netw.*, vol. 2, no. 3, pp. 774–786, Sept. 2018.

[33] Y. Dong, M. J. Hossain, and J. Cheng, "Performance of wireless powered amplify and forward relaying over Nakagami-*m* fading channels with nonlinear energy harvester," *IEEE Commun. Lett.,* vol. 20, no. 4, pp. 672-675, Apr. 2016.

[34] S. Pejoski, Z. Hadzi-Velkov, and R. Schober, "Optimal power and time allocation for WPCNs with piece-wise linear EH model," *IEEE Wireless Commun. Lett.*, vol. 7, no. 3, pp. 364-367, Jun. 2018.

[35] Q. Wu, and R. Zhang, "Towards smart and reconfigurable environment: Intelligent reflecting surface aided wireless network," *IEEE Commun. Mag.*, vol. 58, no. 1, pp. 106-112, Jan. 2020.

[36] K. Shen, and W. Yu, "Fractional programming for communication systems – Part I: power control and beamforming, " *IEEE Trans. Signal Process.*, vol. 66, no. 10, pp. 2616-2630, May, 2018.

[37] K. Shen, and W. Yu, "Fractional Programming for Communication Systems – Part II: Uplink Scheduling via Matching," *IEEE Trans. Signal Process.*, vol. 66, no. 10, pp. 2631-2644, 15, 2018.

[38] H. Guo, Y. Liang, J. Chen, and E. G. Larsson, "Weighted sum-rate maximization for intelligent reflecting surface enhanced wireless networks," in *Proc. IEEE Global Commun. Conf. (GLOBECOM)*, Waikoloa, HI, USA, Dec. 2019, pp. 1-6.

[39] K. Wang, A. M. So, T. Chang, W. Ma, and C. Chi, "Outage constrained robust transmit optimization for multiuser MISO downlinks: tractable approximations by conic optimization," *IEEE Trans. Signal Process.*, vol. 62, no. 21, pp. 5690-5705, Nov. 2014.

[40] H. Guo, Y. Liang, J. Chen, and E. G. Larsson, "Weighted sum-rate maximization for reconfigurable intelligent surface aided wireless networks," *IEEE Trans. Wireless Commun.*,, vol. 19, no. 5, pp. 3064-3076, May 2020.

Sai Xu (Member, IEEE) received the B.S. degree from Hebei Normal University, Shijiazhuang, China, in 2012, and the M.E. and Ph.D. degrees from the Harbin Institute of Technology (HIT), Harbin, China, in 2015 and 2020, respectively. He was also a joint Ph.D. student with the Electrical Engineering Department, University of California, Los Angeles, CA, USA, from October 2017 to April 2019. He is currently an Associate Professor with the School of Cybersecurity, Northwestern Polytechnical University, Xi'an, China, and also a Marie Curie Research Fellow in the Department of Electronic and Electrical Engineering of The University of Sheffield. His research interests include but not limited to intelligent reflecting surface, physical layer security, and 5G/6G communications.

Yanan Du (Graduate Student Member, IEEE) received the B.S. degree from Hebei Normal University, Shijiazhuang, China, in 2012 and the M.S. degree from South China Normal University, Guangzhou, China, in 2015. She was a Joint Ph.D. Student with the Electrical Engineering Department, University of California, Los Angeles, CA, USA, from October 2017 to April 2019. She is currently pursuing the Ph.D. degree with the College of Intelligent Systems Science and Engineering, Harbin Engineering University. Her research interests include cyber-physical systems, physical layer security, and wireless communications.

Jiajia Liu (Senior Member, IEEE) received the B.S. degree in computer science from the Harbin Institute of Technology, Harbin, China, in 2004, the M.S. degree in computer science from Xidian University, Xi'an, China, in 2009, and the Ph.D. degree in information sciences from Tohoku University, Sendai, Japan, in 2012. He is currently a Full Professor (Vice Dean) with the School of Cybersecurity, Northwestern Polytechnical University, Xi'an, China. His research interests include intelligent and connected vehicles, mobile/edge/cloud computing and storage, Internet of things security, wireless and mobile ad hoc networks, and space-air-ground integrated networks.

Jingtao Li received the B. E. degree in 2002 and M.S. degree in 2004, both from the Beijing Institute of Technology, Beijing, China. He is currently a Professor at the Institute of Telecommunication and Navigation Satellites, China Academy of Space Technology, Beijing, China. His research interests include wireless communication, satellite link, communication satellite system, etc.